JACS
JOURNAL OF THE AMERICAN CHEMICAL SOCIETY
Communication
pubs.acs.org/JACS

Absolute and Direct MicroRNA Quantification Using DNA–Gold Nanoparticle Probes

Federica Degliangeli, Prakash Kshirsagar, Virgilio Brunetti, Pier Paolo Pompa,* and Roberto Fiammengo*

Center for Biomolecular Nanotechnologies@UniLe, Istituto Italiano di Tecnologia (IIT),Via Barsanti, 73010 Arnesano, Lecce, Italy

Supporting Information

ABSTRACT: DNA–gold nanoparticle probes are implemented in a simple strategy for direct microRNA (miRNA) quantification. Fluorescently labeled DNA-probe strands are immobilized on PEGylated gold nanoparticles (AuNPs). In the presence of target miRNA, DNA–RNA heteroduplexes are formed and become substrate for the endonuclease DSN (duplex-specific nuclease). Enzymatic hydrolysis of the DNA strands yields a fluorescence signal due to diffusion of the fluorophores away from the gold surface. We show that the molecular design of our DNA–AuNP probes, with the DNA strands immobilized on top of the PEG-based passivation layer, results in nearly unaltered enzymatic activity toward immobilized heteroduplexes compared to substrates free in solution. The assay, developed in a real-time format, allows absolute quantification of as little as 0.2 fmol of miR-203. We also show the application of the assay for direct quantification of cancer-related miR-203 and miR-21 in samples of extracted total RNA from cell cultures. The possibility of direct and absolute quantification may significantly advance the use of microRNAs as biomarkers in the clinical praxis.

MicroRNAs (miRNAs), single-strand noncoding RNAs with a typical length of 21–23 nucleotides, take part as regulatory factors in a number of biological processes via repression of mRNA translation.[1] Alterations in the expression levels of human miRNAs are associated with a variety of pathological conditions including cancer.[2,3] Thus, the actual expression level of one or, more commonly, of several miRNAs may serve as an important diagnostic and prognostic marker. The two most prominent strategies to measure aberrant miRNA expression levels are quantitative RT-PCR (qRT-PCR)[4−6] and oligonucleotide microarrays.[7−9] In addition, alternative technologies, e.g., next-generation sequencing,[10] are being developed.[11] Only few strategies based on nanoparticles have been reported. In 2006 Corn and co-workers reported an array platform for the detection of miRNA, after hybridization and polyadenylation, using a universal DNA-functionalized AuNP.[12] The idea of a universal DNA-functionalized AuNP as a reporter of miRNA hybridization on an array was further developed by Mirkin and co-workers. They recently reported a scanometric miRNA array, which was used to analyze the miRNA profiles of samples from men with prostate cancer.[13] A very interesting assay design was presented by Zhang et al., who combined a two-stage exponential amplification reaction (EXPAR) with a single-quantum-dot based nanosensor and fluorescence detection to reach a 0.1 aM detection limit.[14] However, no application of the reported assay to samples of biological origin was reported. Other very sensitive miRNA detection assays were developed on the basis of the fluorescence arising from DNA-scaffolded silver nanoclusters.[15,16] In most of the reported cases, there is good linear relationship between the output signal and the base 10 logarithm of miRNA concentration, indicative of broad dynamic ranges, at the expenses of a reduced capability of appreciating small concentration differences. However, this is an important issue in miRNA quantification where it has been shown that the differences between normal and dysregulated expression levels are often quite small (often ≤10-fold). Furthermore, absolute quantification of miRNAs still remains challenging, and results may significantly vary depending on the used method/technology.[17] In fact, miRNAs expression levels are frequently normalized to an internal reference, despite this being a controversial issue,[6] and relative miRNA levels are difficult to compare between different studies, a situation that may undermine the wide applicability of miRNA-based diagnosis and prognosis in the clinical praxis.

We introduce here a sensitive assay for the absolute quantification of miRNAs based on enzymatic processing of DNA-functionalized gold nanoparticles (AuNPs), with concomitant development of a fluorescence signal. As little as 0.2 fmol of miRNA can be detected in total RNA extract from cell cultures in 5 h (corresponding to 5 pM miRNA in the assay mixture). The assay is direct, i.e., does not require the conversion of miRNA into cDNA, and no target amplification steps are needed. For assay development, we have chosen two microRNAs, namely, hsa-miR-21 and hsa-miR-203, representing high- and low-abundance miRNAs, respectively.[18] miR-21 is abundant and overexpressed in almost all tumor tissues,[19] while miR-203 is practically absent in most organs[18,20] with the exception of skin and the esophagus, where it is found at relatively high levels.

The assay strategy is illustrated in Scheme 1. Fluorescently labeled DNA probes are immobilized on the passivation layer of PEGylated AuNPs, and fluorescence is efficiently quenched by the vicinity of the fluorophores to the AuNP surface.[21] In presence of target miRNA, DNA–RNA heteroduplexes are formed and can be hydrolyzed by the duplex-specific nuclease (DSN) enzyme. As a result, fluorophores are released in solution, resulting in the appearance of a fluorescence signal.

Received: December 10, 2013
Published: February 3, 2014

dx.doi.org/10.1021/ja412152x | J. Am. Chem. Soc. 2014, 136, 2264–2267

Scheme 1. Assay Strategy

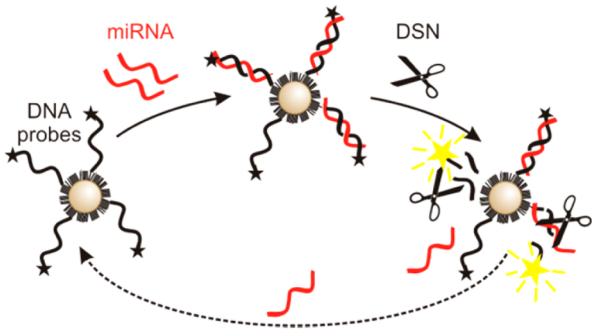

DSN: Duplex-specific nuclease

DSN is a highly stable, nonspecific endonuclease, which possesses strong preference for double stranded DNA and DNA in DNA–RNA heteroduplexes.[22] The substrate specificity of this enzyme is ideal for the development of miRNA sensing strategies.[23−25] Since miRNA strands (target) remain intact during this process, under conditions of effective enzymatic activity, target-recycling amplification leads to significant signal enhancement (vide infra).

The DNA–AuNP probes were prepared following a strategy that we have previously developed for the conjugation of negatively charged peptides to PEGylated AuNPs.[26] Shortly, citrate-capped AuNPs were passivated with mixed-monolayers of ω-carboxy- and ω-amino-polyethylene glycol (PEG-600) thiols. Successively 5′-FAM-labeled oligonucleotides were coupled via their 3′-thiol to the primary amino groups on the passivation layer using a hetero-bifunctional linker. We obtained very stable DNA–AuNP conjugates with multiple oligonucleotide probe sequences per AuNP. Three AuNP sizes were selected for our studies with nominal diameter of 40, 13, and 5 nm (referring to the Au core, Table 1).

Table 1. Size (Diameter) and Functionalization of DNA–AuNP Probes

nominal size (nm)	Au core (nm)[a]	hydrodyn size (nm)[b]	DNA/AuNP[c]
40	37 ± 3	65 ± 12	110 ± 16[d]
	37 ± 3	60 ± 15	103 ± 15[e]
13	13 ± 2	18 ± 3	26 ± 4[d]
5	6 ± 2	–	3 ± 1[d]

[a]Measured by TEM. [b]Measured by DLS. [c]Batch to batch variability from at least two independent preparations. [d]DNA = Probe_203 (DNA probe for miR-203; for sequence, see Supporting Information). [e]DNA = Probe_21.

As proof of principle, we initially confirmed that the assay strategy was working by observing the appearance of a fluorescence signal when DSN was added to mixtures of 40 nm DNA–AuNP probes and synthetic miR-203. The fluorescence increased for approximately 2 h before reaching a plateau (Figure 1a) corresponding to complete digestion of all immobilized probe strands, irrespective of the initial miRNA amount being in excess (5 equiv) or in defect (0.2 equiv). This outcome indicates that only the DNA probe strands of the immobilized heteroduplexes are efficiently hydrolyzed by DSN, while target miRNA is not degraded and can rehybridize several times until complete probe degradation is achieved (here 5 times). The blank reaction, missing the miRNA target, showed in comparison only a very marginal increase in fluorescence

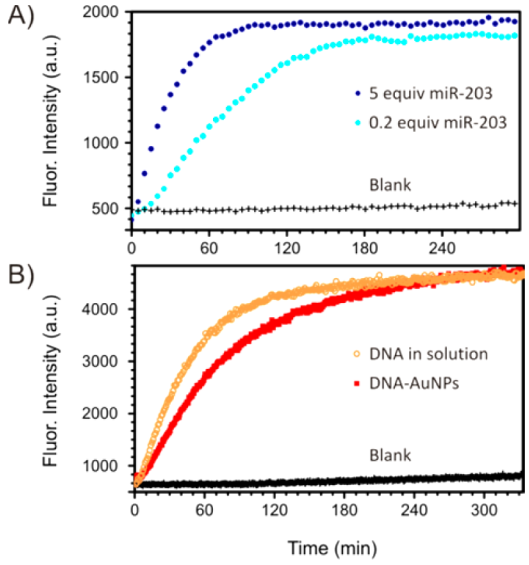

Figure 1. Enzymatic processing of DNA–AuNP probes. (A) Target recycling: complete DNA hydrolysis is reached even in defect of target miRNA; 19 pM of 40 nm AuNPs (110 DNA/AuNP), 0.02 U/μL of DSN, 20 mM Mg^{2+}, 0.2 or 5 equiv of target miR-203 (400 pM and 10 nM, respectively). (B) Hydrolysis of DNA on AuNPs is only 1.7 times slower than in solution; 50 pM of 13 nm AuNPs (26 DNA/AuNP) corresponding to 1.3 nM free DNA (probe_203) in solution, 0.005 U/μL of DSN, 20 mM Mg^{2+}, 15 nM target miR-203.

signal, due to the low activity of DSN toward single stranded DNA (the probes). It is important to note that our DNA–AuNPs remain stable in the assay buffer containing 1 mM of dithiothreitol (DTT, necessary for optimal enzymatic activity) for over 10 h at 42 °C. This observation justifies our specific DNA–AuNP design strategy. In fact, although more straightforward, direct immobilization of thiol-modified DNA strands on the gold surface affords nanoparticles of marginal stability under these conditions,[27] with significant release of the probes even in absence of DSN.

After having demonstrated that the proposed detection strategy works, we set out to investigate whether the enzymatic activity of DSN was negatively affected by immobilization of the oligonucleotides on the nanoparticle surface. Mirkin and co-workers have shown that DNase I and other aspecific serum nucleases are significantly inhibited when oligonucleotides are immobilized on AuNPs.[28] This property constitutes one of the basis for success of the so-called "spherical nucleic acids" (SNA).[29] It most probably originates from the low tolerance of many nucleases toward the high ionic strength conditions found at the nanoparticle surface.[28] Although the DNA–AuNP conjugates reported here have a very different molecular design compared to SNA, they still are polyanionic due to the carboxyl-terminated PEG-thiol in the passivation shell. Furthermore, DSN is also reported to be highly sensitive to the ionic strength of the medium, with a 10-fold decrease in catalytic activity in the presence of 0.2 M NaCl.[22] Given these two premises, we reasoned it was mandatory to compare DNS activity on substrates in solution and on the AuNPs. A model system in solution was created hybridizing the same 5′-FAM labeled DNA sequence used for AuNP functionalization with a complementary 3′-Dabcyl-miRNA (the target sequence). The enzymatic activity of DSN on the AuNP-immobilized substrates vs substrates in solution was compared at equal probe and target concentrations (Figure 1b). Interestingly, the initial

dx.doi.org/10.1021/ja412152x | J. Am. Chem. Soc. 2014, 136, 2264−2267

reaction rate for immobilized substrates (heteroduplexes on the AuNPs) was only 1.7-fold lower than for substrates in solution, allowing us to exploit the activity of DSN at its best. Furthermore, identical behavior was obtained for 13 nm as well as for 40 nm DNA−AuNPs (see Figure S5, Supporting Information). Most importantly, no significant differences in hydrolysis rate were observed when the assay was performed with DNA−AuNP probes of different size at fixed DNA-probe concentration (1.3 nM) (see Figure S7, Supporting Information). DSN is thus able to process the immobilized heteroduplexes equally well, irrespective of AuNP size. This result indicates that the specific design of our DNA−AuNPs, with the DNA probe strands anchored to the PEG-based passivation layer, guarantees excellent accessibility of the immobilized heteroduplex, a highly desired property for the development of efficient biosensors.

Next we investigated the effect of AuNP size on the intensity of the developed fluorescence signal. It is well-known that AuNPs very efficiently quench the fluorescence of fluorophores immobilized on their surface.[21,30] This phenomenon occurs even for very small AuNPs (<5 nm).[31,32] We observed efficient fluorophore quenching for all investigated DNA−AuNPs, as demonstrated by the large fluorescence intensity increase caused by DSN digestion, which is not depending on nanoparticle size provided that the DNA-probe concentration is fixed (e.g., Figure S7, Supporting Information, 40 and 5 nm AuNPs). However, since AuNPs > 2 nm possess a plasmon resonance whose intensity scales as the third power of nanoparticle's diameter, the signal intensity may be thwarted due to trivial absorption of fluorescence as well as of excitation light.[21] The magnitude of this effect is directly proportional to nanoparticle concentration and is expected to be low in our assay (AuNP concentration generally ≤50 pM for the largest AuNPs). This was experimentally confirmed by showing that the sensitivity of fluorescence detection, defined as the slope of the line fluorescence intensity vs fluorophore concentration under the assay conditions, is marginally reduced (1.2-fold) only for 40 nm DNA−AuNPs, while no effect is observed for 13 and 5 nm DNA−AuNPs (see Supporting Information). Larger nanoparticles are however preferable because their concentration can be more precisely estimated.

Under optimized test conditions (40 μL of assay mixture, 2 nM DNA-probe, 0.02 U/μL of DSN, 37 °C) very good linear response is observed in the range between 5 and 200 pM of miRNA concentration (see Figure 2) after 2 h incubation. Longer assay times, e.g., 5 h, improve the signal for miRNA concentrations below 25 pM. The limit of detection (LoD) was estimated taking miR-203 as the model miRNA because its abundance is generally low, except for skin. Three different approaches were used for the estimate according to the definition suggested by different standardization organizations (see Supporting Information). The LoD was found to be between 5 and 8 pM (or 0.2−0.3 fmol) miRNA after 5 h, depending on the chosen approach, and the presence of total RNA in the assay mixture did not affect quantification. Here it is important to note that target-recycling amplification (vide supra) cannot per se improve the LoD of a sensing strategy, which is instead controlled by the catalytic efficiency of the enzyme.[33] In other words, at low miRNA concentrations approaching the detection limit, probe DNA is in large excess and practically constant, and target recycling only guarantees a constant, but low, substrate concentration. Thus, a lower LoD can only be obtained using a faster enzyme.

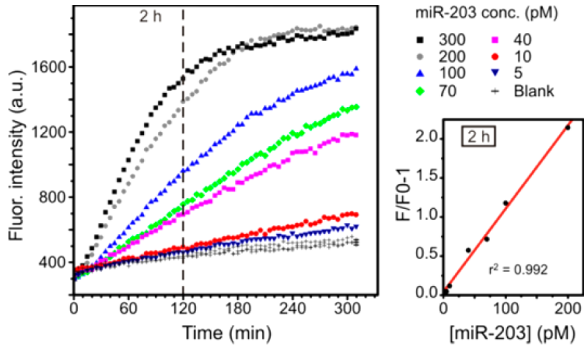

Figure 2. Real-time monitoring of assay mixtures containing different miRNA concentrations. The relastionship between fluorescence signal and miRNA concentration after 2 h is linear. 17 pM of 40 nm AuNPs (110 DNA/AuNP), 0.02 U/μL of DSN, 20 mM Mg^{2+}, 0.5 U/μL of RNase inhibitor, 37 °C.

Nevertheless, the LoD of our assay is actually more than sufficient for quantification of "real samples" according to recent literature reports. In fact, a low abundance sample such as total RNA extracted from CD34(+)/CD133(−) hematopoietic stem cells, has individual miRNA amount with a median of 0.3 fmol/10 μg of total RNA (or 0.3 fmol/10^6 cells) practically at the LoD of our assay, while total RNA from mouse liver contains 10-times more miRNA.[9]

Finally, we proved the performance of our assay by measuring the absolute amounts of miR-203 and miR-21 in cancerous cell lines. Total RNA was extracted from MCF7 (human breast adenocarcinoma), KYSE270 (human esophageal squamous cell carcinoma), and HeLa (human epitheloid cervix carcinoma) cells. The experimental conditions for the assay on total RNA samples were fine-tuned by bringing the assay temperature to 42 °C and by addition of NaCl (final concentration 50 mM). miRNA quantification resulted in the amounts reported in Table 2. Notably, we found it was not

Table 2. miRNA Amounts (Copies/ng_{RNA} × 10^4) in Extracted Total RNA from Cell Cultures[a]

miRNA	MCF7	KYSE270	HeLa
hsa-miR-203[b]	4.0 ± 1.2	2.1 ± 1.1	<1
hsa-miR-21[c]	75 ± 43	30 ± 8	24 ± 1

[a]10 μg of total RNA per assay; data are averages ± SD of three independent experiments. [b]Assay time 5 h. [c]Assay time 2 h.

possible to apply the assay directly on Trizol-based cellular lysates (after 10 times dilution), most probably because of denaturation of DSN under these conditions. A control experiment with spiked miR-203 in a HeLa lysate (40 pM final concentration in the assay mixture) showed indeed very little DSN activity (~25%, Table S3, Supporting Information). Our results confirmed the higher abundance of miR-21 compared to mir-203. The absolute amounts of miR21 are ≥10 times higher than those of miR-203 in all investigated cell lines, confirming that this miRNA is in general highly expressed in almost all cancer types. In particular, the amount of miR21 found in MCF7 cells (7.5 × 10^5 copies/ng_{RNA} or 1.2 amol/ng_{RNA}) agrees well with the values reported by Chan and coworkers (0.92 amol/ng_{RNA}) using a TIRF-microscopy-based assay additionally validated by qRT-PCR,[34] demonstrating the reliability of our assay. miR-203 was detected only in KYSE270 cells[35] and in MCF7 cells.[36] Considering a typical value of 10

dx.doi.org/10.1021/ja412152x | J. Am. Chem. Soc. 2014, 136, 2264−2267

pg of total RNA/cell, the amounts of miR-203 were 210 and 400 copies/cell in KYSE270 and MCF7 cells, respectively. HeLa total RNA did not contain any detectable amount of miR-203 by our assay; i.e., these cells express less than approximately 1×10^4 miR-203 copies/ng_{RNA} or 100 copies/cell, which corresponds to the method detection limit (MDL, see Supporting Information) when the assay is performed on 8−12 μg of total RNA extracted from cultured cells using Trizol reagent. This result is consistent with previous observations indicating that HeLa cells have indeed very low miR-203 levels.[37,38]

In conclusion, the developed assay is able to quantify the absolute amount of miRNA in extracted total RNA down to 1×10^4 copies/ng_{RNA} (or 100 copies/cell) in samples of 8−12 μg of total RNA (approximately 10^6 cells). The assay is direct, not requiring the conversion of target miRNA into cDNA, and it is technologically easy to implement since thermal cycling is not needed. The assay strategy is general enough to be extended to the parallel quantification of a selected panel of miRNAs relevant to a given pathology identified by, e.g., microarray screening.

■ ASSOCIATED CONTENT

Supporting Information

Description of materials, methods, and full experimental procedures. This material is available free of charge via the Internet at http://pubs.acs.org.

■ AUTHOR INFORMATION

Corresponding Authors

roberto.fiammengo@iit.it
pierpaolo.pompa@iit.it

Notes

The authors declare no competing financial interest.

■ ACKNOWLEDGMENTS

This work was partially supported by the Italian Flagship Project NanoMax. The authors thank Dr. M. Malvindi for TEM measurements and Dr. P. Valentini and Dr. J. H. Kim for insightful discussions.

■ REFERENCES

(1) Almeida, M. I.; Reis, R. M.; Calin, G. A. *Mutat. Res., Fundam. Mol. Mech. Mutagen.* **2011**, *717*, 1.
(2) Di Leva, G.; Croce, C. M. *Curr. Opin. Genet. Dev.* **2013**, *23*, 3.
(3) Farazi, T. A.; Spitzer, J. I.; Morozov, P.; Tuschl, T. *J. Pathol.* **2011**, *223*, 102.
(4) Chen, C.; Ridzon, D. A.; Broomer, A. J.; Zhou, Z.; Lee, D. H.; Nguyen, J. T.; Barbisin, M.; Xu, N. L.; Mahuvakar, V. R.; Andersen, M. R.; Lao, K. Q.; Livak, K. J.; Guegler, K. J. *Nucleic Acids Res.* **2005**, *33*, e179.
(5) Benes, V.; Castoldi, M. *Methods* **2010**, *50*, 244.
(6) Redshaw, N.; Wilkes, T.; Whale, A.; Cowen, S.; Huggett, J.; Foy, C. A. *Biotechniques* **2013**, *54*, 155.
(7) Git, A.; Dvinge, H.; Salmon-Divon, M.; Osborne, M.; Kutter, C.; Hadfield, J.; Bertone, P.; Caldas, C. *RNA* **2010**, *16*, 991.
(8) Jensen, S. G.; Lamy, P.; Rasmussen, M. H.; Ostenfeld, M. S.; Dyrskjøt, L.; Ørntoft, T. F.; Andersen, C. L. *BMC Genomics* **2011**, *12*, 435.
(9) Bissels, U.; Wild, S.; Tomiuk, S.; Holste, A.; Hafner, M.; Tuschl, T.; Bosio, A. *RNA* **2009**, *15*, 2375.
(10) Hafner, M.; Landgraf, P.; Ludwig, J.; Rice, A.; Ojo, T.; Lin, C.; Holoch, D.; Lim, C.; Tuschl, T. *Methods* **2008**, *44*, 3.
(11) Dong, H.; Lei, J.; Ding, L.; Wen, Y.; Ju, H.; Zhang, X. *Chem. Rev.* **2013**, *113*, 6207.
(12) Fang, S.; Lee, H. J.; Wark, A. W.; Corn, R. M. *J. Am. Chem. Soc.* **2006**, *128*, 14044.
(13) Alhasan, A. H.; Kim, D. Y.; Daniel, W. L.; Watson, E.; Meeks, J. J.; Thaxton, C. S.; Mirkin, C. A. *Anal. Chem.* **2012**, *84*, 4153.
(14) Zhang, Y.; Zhang, C.-y. *Anal. Chem.* **2011**, *84*, 224.
(15) Liu, Y.-Q.; Zhang, M.; Yin, B.-C.; Ye, B.-C. *Anal. Chem.* **2012**, *84*, 5165.
(16) Yang, S. W.; Vosch, T. *Anal. Chem.* **2011**, *83*, 6935.
(17) Leshkowitz, D.; Horn-Saban, S.; Parmet, Y.; Feldmesser, E. *RNA* **2013**, *19*, 527.
(18) Sonkoly, E.; Wei, T.; Janson, P. C. J.; Sääf, A.; Lundeberg, L.; Tengvall-Linder, M.; Norstedt, G.; Alenius, H.; Homey, B.; Scheynius, A.; Ståhle, M.; Pivarcsi, A. *PLoS One* **2007**, *2*, e0000610.
(19) Krichevsky, A. M.; Gabriely, G. *J. Cell. Mol. Med.* **2009**, *13*, 39.
(20) Jackson, S. J.; Zhang, Z.; Feng, D.; Flagg, M.; O'Loughlin, E.; Wang, D.; Stokes, N.; Fuchs, E.; Yi, R. *Development* **2013**, *140*, 1882.
(21) Dulkeith, E.; Ringler, M.; Klar, T. A.; Feldmann, J.; Muñoz Javier, A.; Parak, W. J. *Nano Lett.* **2005**, *5*, 585.
(22) Anisimova, V.; Rebrikov, D.; Shagin, D.; Kozhemyako, V.; Menzorova, N.; Staroverov, D.; Ziganshin, R.; Vagner, L.; Rasskazov, V.; Lukyanov, S.; Shcheglov, A. *BMC Biochem.* **2008**, *9*, 14.
(23) Ren, Y.; Deng, H.; Shen, W.; Gao, Z. *Anal. Chem.* **2013**, *85*, 4784.
(24) Yin, B.-C.; Liu, Y.-Q.; Ye, B.-C. *J. Am. Chem. Soc.* **2012**, *134*, 5064.
(25) Tian, T.; Xiao, H.; Zhang, Z.; Long, Y.; Peng, S.; Wang, S.; Zhou, X.; Liu, S.; Zhou, X. *Chem.—Eur. J.* **2013**, *19*, 92.
(26) Maus, L.; Dick, O.; Bading, H.; Spatz, J. P.; Fiammengo, R. *ACS Nano* **2010**, *4*, 6617.
(27) Li, Z.; Jin, R.; Mirkin, C. A.; Letsinger, R. L. *Nucleic Acids Res.* **2002**, *30*, 1558.
(28) Prigodich, A. E.; Alhasan, A. H.; Mirkin, C. A. *J. Am. Chem. Soc.* **2011**, *133*, 2120.
(29) Cutler, J. I.; Auyeung, E.; Mirkin, C. A. *J. Am. Chem. Soc.* **2012**, *134*, 1376.
(30) Swierczewska, M.; Lee, S.; Chen, X. *Phys. Chem. Chem. Phys.* **2011**, *13*, 9929.
(31) Dulkeith, E.; Morteani, A. C.; Niedereichholz, T.; Klar, T. A.; Feldmann, J.; Levi, S. A.; van Veggel, F. C. J. M.; Reinhoudt, D. N.; Möller, M.; Gittins, D. I. *Phys. Rev. Lett.* **2002**, *89*, 203002.
(32) Jennings, T. L.; Singh, M. P.; Strouse, G. F. *J. Am. Chem. Soc.* **2006**, *128*, 5462.
(33) Fang, S.; Lee, H. J.; Wark, A. W.; Kim, H. M.; Corn, R. M. *Anal. Chem.* **2005**, *77*, 6528.
(34) Chan, H.-M.; Chan, L.-S.; Wong, R. N.-S.; Li, H.-W. *Anal. Chem.* **2010**, *82*, 6911.
(35) Ikenaga, N.; Ohuchida, K.; Mizumoto, K.; Yu, J.; Kayashima, T.; Sakai, H.; Fujita, H.; Nakata, K.; Tanaka, M. *Ann. Surg. Oncol.* **2010**, *17*, 3120.
(36) Yu, X.; Zhang, X.; Dhakal, I.; Beggs, M.; Kadlubar, S.; Luo, D. *BMC Cancer* **2012**, *12*, 29.
(37) Zhu, X.; Er, K.; Mao, C.; Yan, Q.; Xu, H.; Zhang, Y.; Zhu, J.; Cui, F.; Zhao, W.; Shi, H. *Cell. Physiol. Biochem.* **2013**, *32*, 64.
(38) Hemida, M. G.; Ye, X.; Zhang, H. M.; Hanson, P. J.; Liu, Z.; McManus, B. M.; Yang, D. *Cell. Mol. Life Sci.* **2013**, *70*, 277.